Symmetry Considerations for Closed Loop Photonic Crystal Coupled Resonators

Matthew D. Weed, *Student Member, IEEE*, Charles G. Williams, *Student Member, IEEE*, Peter J. Delfyett, *Fellow, IEEE*, and Winston V. Schoenfeld, *Member, IEEE*

***Abstract*—Waveguide coupling to closed loop coupled-resonator optical waveguides is explored. By coupling a CROW chain back on itself, a reduction in individual resonant linewidth is achieved making these slow light modes more conducive to periodic filters toward novel frequency-comb integration. Through numerical simulation by finite-difference time-domain methods, the importance of waveguide symmetry conditions for coupling is illustrated. The impact of unit cavity mode symmetry strongly impacts the necessary coupling geometry to both cavities and waveguides. Design insight into different waveguide coupling schemes is provided while aiming to achieve transmission of the resonant structure exhibited by the isolated resonator.**

***Index Terms*—Integrated optics, mode matching methods, optical resonators, resonator filters.**

I. Introduction

In the field of photonics, both active and passive devices demand high finesse resonances for mode selectivity, stability, or resonant shift sensitivity. Passive devices such as environmental sensors and spectral filters make use of high finesse resonances to increase their sensitivity [1]–[4]; micro-laser designs look to minimize resonant linewidth and lasing threshold [5]–[9]; hybrid devices like those that make up communications systems value linewidth and stability toward a more dense communication architecture [10]–[12]. In addition to higher finesse, continually smaller form-factors are desirable. This second demand comes into direct conflict with the first due to the long photon lifetimes in long cavities normally necessary to achieve fine linewidth. Fortunately, through the use of micro-rings and photonic crystal cavities, there exists the potential to satisfy both demands simultaneously.

Slow-light in an integrated, chip-level manifestation has become the topic of intense study in recent years. As the fabrication quality of features on the sub-wavelength scale and side-wall roughness has improved, weight has been given to the claims of optical systems such as micro-ring resonators and photonic crystals [10], [13]–[18]. In these devices, waveguide dispersion is used to generate optical modes with low group velocity. This slow-light effect therefore enhances temporal light-matter interactions, enabling dramatic reductions in device scale. Coupled-resonator optical waveguides (CROWs) have been shown to offer strong slow-light potential, as well as large group velocity dispersion and a multi-resonant modal structure that can be readily manipulated by design [19]. The CROW technique has been extensively studied using micro-rings as the unit cavity but has also been extended to photonic crystal cavities. In both cases, the unit-cavity Q factor is preserved with the addition of coupled cavities [17], [20]. While the fabrication quality of micro-rings is currently superior to photonic crystal systems due to less field interaction with etched-edge roughness, the benefits in scale, field confinement, and propensity for integration motivates this work in pursuit of a photonic crystal embodiment of CROWs.

Traditionally, spectral composition of CROW devices has been studied without much interest in the finer modal structure available in a given resonant window. Instead, they have been explored for their dispersion characteristics and use as filters, pulse shapers, and delay lines [21]–[23]. It is proposed here that if these split resonant modes of CROW lines could be made to exhibit very narrow linewidths, their application space could be greatly expanded. Toward this goal, we previously presented the design of a CROW chain that loops back on itself, a coupled-resonator optical waveguide loop (CROWL) [24]. This design takes a cue from the work of Poon *et al.*, and is capable of offering a resonant structure unique from its open chain counterpart with increased finesse [25]. These circularly arrayed architectures have been primarily studied with regard to rotation sensors but also may have future applications in tunable laser sources [25]–[30]. CROWLs are explored further in this paper with a focus on coupling methods for the insertion of light into, and extraction of light out of such devices. An investigation into the modal structure of a six-cavity CROWL was carried out to illuminate the three photonic crystal waveguide-to-cavity coupling geometries explored.

II. CROW Background and Theory

When cavities are brought in close proximity to each other, light that was once confined to a single cavity is allowed to evanescently couple between them. The isolated cavity's single frequency resonance takes on a sinusoidal dispersion relation as shown in Fig. 1 that is indicative of wave propagation. This guided wave is referred to as a CROW mode. A transmission filter made up of N coupled resonators, where N is finite, results in a spectrum of N peaks with frequencies corresponding to evenly spaced k-values, as illustrated in Fig. 1. Conveniently, the two figures of merit that govern this resonant structure,

Manuscript received September 14, 2012; revised January 22, 2013; accepted February 21, 2013. Date of publication March 07, 2013; date of current version March 15, 2013.

The authors are with the College of Optics and Photonics (CREOL), University of Central Florida, Orlando, FL 32816 USA (e-mail: mweed@creol.ucf.edu).

Color versions of one or more of the figures in this paper are available online at http://ieeexplore.ieee.org.

Digital Object Identifier 10.1109/JLT.2013.2250915

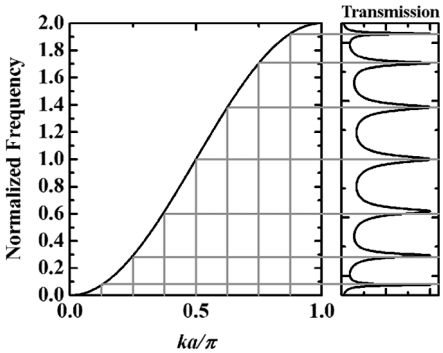

Fig. 1. The dispersion and transmissive mode splitting of an arbitrary CROW chain with seven coupled resonators. Calculated using coupled mode theory.

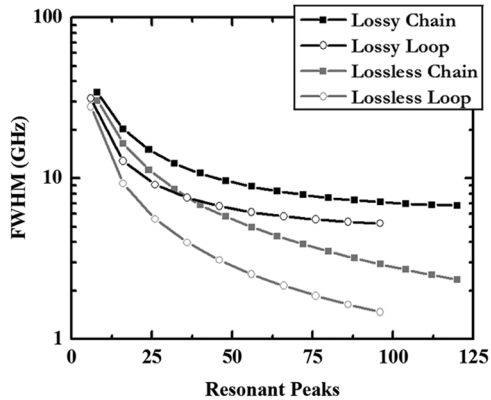

Fig. 2. Coupled mode theory generated scan over CROW and CROWL devices with increasing number of peaks.

peak full-width half-maximum (FWHM) and free spectral range (FSR), can be decoupled and considered separately. Therefore, the designer may engineer them through control over external decay times to waveguides or free-space (loss) (τ), and the inter-cavity coupling constant (κ) respectively [13].

Studying these waveguides using the coupled mode theory (CMT) equation shown below in (1), for a six-cavity CROWL, offers a means for qualitative, and to a limited degree quantitative, analysis of CROW resonant behavior [23], [31]. The full bandwidth of this resonant feature is purely dependent on κ, equal to four times the coefficient, and so scaling this system up to many resonators will result in an increasingly dense set of peaks. The off-diagonal coupling terms (in red) of κ_6 are what makes this coupling matrix periodic and, physically, a loop. (See equation at bottom of page)

If loss, denoted by $1/\tau$ is ignored, both FSR and FWHM drop off as $1/N$ leaving the finesse constant. The inclusion of cavity loss, however, slows the FWHM drop off, shown in Fig. 2, yielding a decreasing finesse with N. The additional feedback mechanism offered in the closed loop geometry promises to help alleviate this trend by imparting consistently finer FWHM.

In order to achieve realistic quantitative analysis of such a system, CMT calculations were abandoned in favor of finite-difference time-domain (FDTD) calculations. A more physically inclusive, albeit more computationally extensive tool, FDTD allows for the simulation of real structures. The calculations that follow were performed by FullWAVE from R-Soft Designs and make use of a TE-like polarization effective index method which allows for significantly less computationally exhaustive 2-D simulations during optimization.

The physical system of choice for this work is based in a photonic crystal backbone that has a hexagonal lattice of circular air holes of radius $0.3 * a$, where a is the lattice constant. Featuring standing mode oscillation when isolated, the cavity that makes this looped architecture possible features preferential field leaking in a 30° cross about the cavity center, as shown in Fig. 3. Referred to as an L3s1 cavity and shown as inset in Fig. 3, the photonic crystal defect consists of three missing air holes and one hole on each end that is shrunk to $2/3 * \mathrm{R}_0$ and shifted outward by $0.2 * a$. The spectral response of this isolated cavity is shown with reference to the spatial mode structure in Fig. 3.

Mode 1 is extensively studied in the literature and couples most strongly along a 30° cross [32]–[34]. This geometry yields a fundamental six-cavity loop geometry of the hexagon shown as inset to Fig. 4. Limited only by this 30° inter-cavity coupling restriction, this unit cavity may be implemented in CROWL resonators that scale larger than the six-cavity example discussed in this work. Loops of $N = 4m + 6$ are possible when m is any integer. The other modes also exhibit similar 30° field strength, but with weaker preference. It should be noted in Fig. 3 mode 2 however, that the field geometry is very similar to that of mode 1. The important difference is that mode 1 is only symmetric about the x axis while mode 2 offers two-fold reflection symmetry, along the x- and z-axis, which may prove useful in future work.

By calculating the resonant response of an isolated six-cavity CROWL in a 3-D slab of GaAs or Si with index 3.4 (Fig. 4), loss parameters are considered and matched to 2-D simulations with great agreement. For the case of TE-like modes in photonic

$$\mathbf{A}\vec{\mathbf{a}} = \begin{bmatrix} s+1/\tau_1 & i\kappa_1 & 0 & 0 & 0 & i\kappa_6 \\ i\kappa_1 & s+1/\tau_2 & i\kappa_2 & 0 & 0 & 0 \\ 0 & i\kappa_2 & s+1/\tau_3 & i\kappa_3 & 0 & 0 \\ 0 & 0 & i\kappa_3 & s+1/\tau_4 & i\kappa_4 & 0 \\ 0 & 0 & 0 & i\kappa_4 & s+1/\tau_5 & i\kappa_5 \\ i\kappa_6 & 0 & 0 & 0 & i\kappa_5 & s+1/\tau_6 \end{bmatrix} \begin{bmatrix} a_1 \\ a_2 \\ a_3 \\ a_4 \\ a_5 \\ a_6 \end{bmatrix} = \begin{bmatrix} -i\mu_{\mathrm{in}} S_{\mathrm{in}} \\ 0 \\ 0 \\ 0 \\ 0 \\ 0 \end{bmatrix} \tag{1}$$

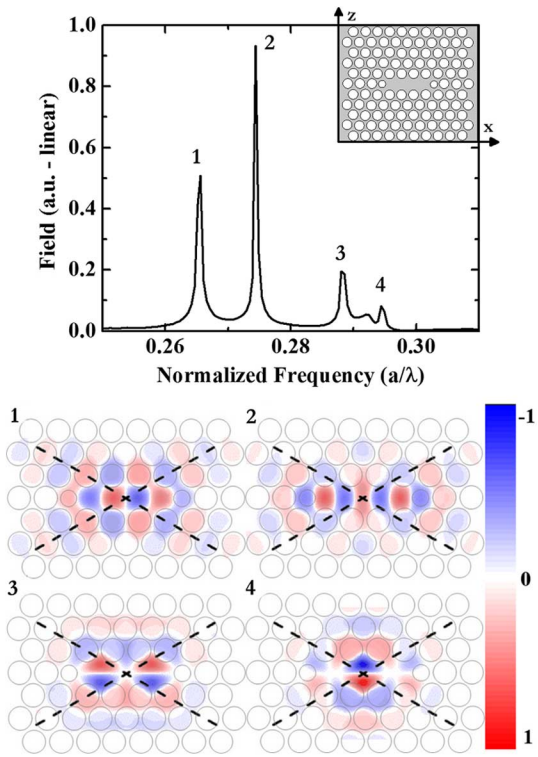

Fig. 3. (color online) FDTD simulation of the L3s1 unit cell defect cavity resonances within the photonic bandgap of a 3-D dielectric slab with index 3.4 and thickness of $0.6 * a$. Also provided are 2D-plane slices of the $\mathbf{H}_y$ mode structures corresponding to these resonances.

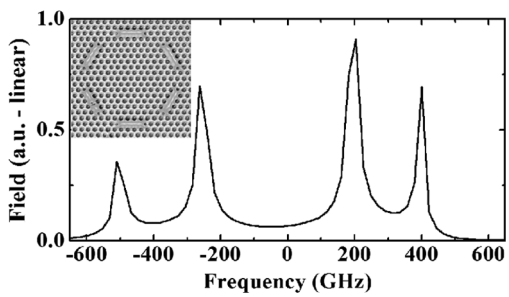

Fig. 4. 3D FDTD calculated resonant spectra of an isolated six-cavity CROWL simulated as air holes in a slab of index 3.4 with resonance centered at 1.55 μm wavelength. Inset shows device illustration.

crystals, this type of effective index method has been shown to be a good approximation [35]. Due to radiation mode coupling, an effective index of 4.0 is found to be appropriate for simulating the resonant structure with regard to linewidth and FSR (Fig. 5(a)). An effective index of 2.77, however, is appropriate for approximating the resonant center frequency in 2-D (Fig. 5(b)). While the resonant center frequency is dependent on the mode of the unit-cell cavity, the coupled-cavity resonant structure is dependent on the coupling parameters between cavities (κ) which, due to expected radiation loss, shows reduced effective inter-cavity coupling. This smaller inter-cavity coupling has the same result on the coupled-cavity resonant structure as raising the cavity's Q. Therefore, raising the index of the material in 2-D serves to mimic these conditions in 3-D for our specific case.

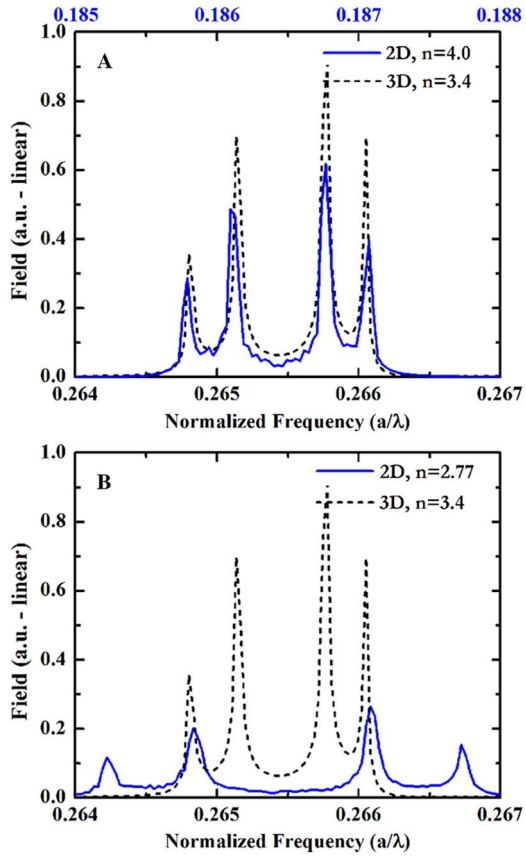

Fig. 5. (color online) Effective index calculations to determine appropriate 2-D indexes to approximate a 3-D photonic crystal slab featuring a CROWL structure. Both calibration for resonant characteristics at; (a) $\mathrm{n_{eff}} = 4.0$ and resonant center at; (b) $\mathrm{n_{eff}} = 2.77$ were performed.

III. Mode Symmetry Results

In an effort to better understand the spatial mode structure of CROWL resonances, the frequency response of an isolated six-cavity CROWL was studied using FDTD simulation. By numerically forcing field symmetry along the two in-plane axes (x and z) via boundary conditions, it becomes clear through inspection of Fig. 6(a) that the four resonances predicted in the CMT model are spatially antisymmetric about the z-axis. It is also illustrated in Fig. 6(a) that there are actually two x-symmetric and two x-antisymmetric resonances that make up the four-peak resonant structure of a six-cavity CROWL.

Next, by numerically forcing spatial symmetry about the z-axis, a single pair of modes is present whose center is red shifted from the single-cavity and z-antisymmetric cases. This z-symmetric set also shows x-symmetric or antisymmetric versions along the same lines as those of z-antisymmetry (Fig. 6(b)). For clarity in identifying resonant symmetry characteristics, the frequency markers shown in Fig. 6 will be reproduced on the subsequent analyses of CROWL coupling geometries.

To further illustrate the structure of these modes, Fig. 7 shows a simplified picture of how an isolated cavity mode like that of mode 1 (Fig. 3) with Z-antisymmetry would resonate in a six-cavity CROWL system like that under investigation here.

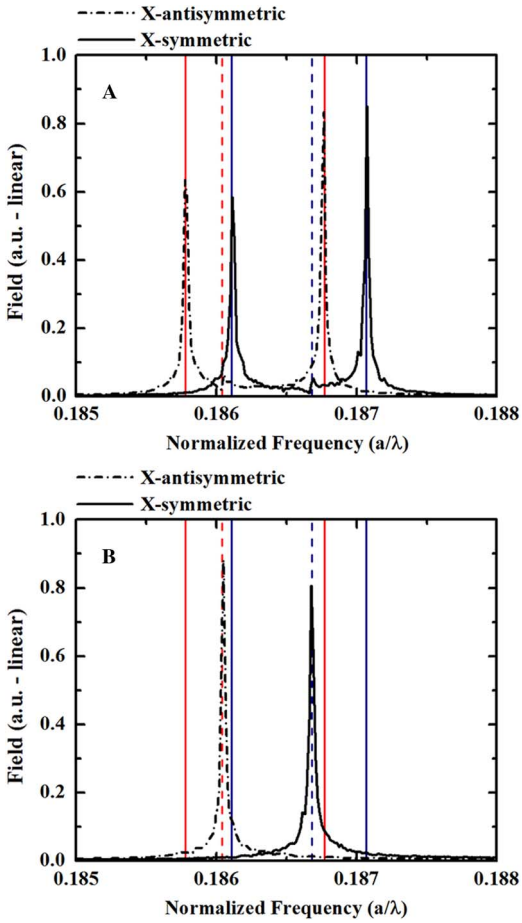

Fig. 6. (color online) Spectral response of an isolated six-cavity CROWL under symmetry restricting simulation with (a) Z-antisymmetry and (b) Z-symmetry. Solid and dashed frequency markers indicate Z-antisymmetric and Z-symmetric resonances, respectively. Red and blue frequency markers indicate X-antisymmetric and X-symmetric resonances, respectively.

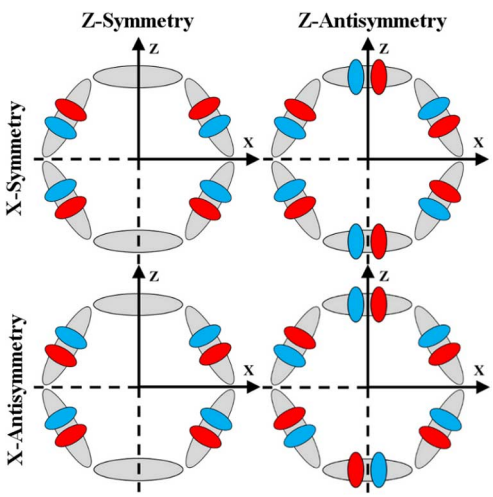

Fig. 7. (color online) Illustration of a six-cavity CROWL showing mode structure symmetries. Red and blue regions represent respectively positive or negative $\mathbf{H}_y$ field direction. Empty cavities are necessary to exhibit Z-symmetry.

IV. CROWL Coupling Results

Our previous work focused on a waveguide coupling scheme attempting to best match the unit resonator mode's geometry, a

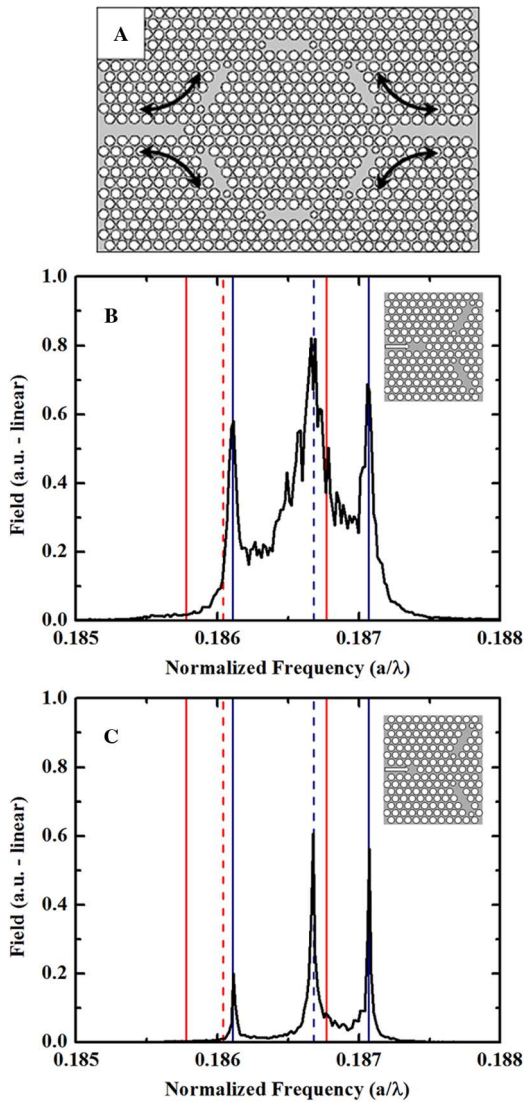

Fig. 8. (color online); (a) Schematic of symmetric butt-coupling technique for accessing a photonic crystal CROWL. FDTD transmission for a waveguide end to cavity center distance of; (b) $6.08a$ and (c) $6.93a$.

30° cross. The result is what will be called symmetric butt-coupling and is illustrated in Fig. 8(a) with introduction in [24]. From the above symmetry study, however, a weakness of this coupling method was observed. Symmetrically coupling to two cavities simultaneously forces X-symmetry in the CROWL resonator and limits the modes allowed to transmit. Therefore, the following is intended to identify a waveguide coupling scheme capable of transferring the Z-Antisymmetric modes this CROWL exhibits in isolation from waveguides. Additionally, we wish to maximize resonant finesse where possible.

It was observed that the spectral response of our unit cavity is distorted when the waveguide is brought too close to a cavity. Therefore, in this symmetric butt-coupling scheme, the CROWL under study yields resonant features that are recognizable when the input waveguide is moved to $6.08 * \mathrm{a}$ from the targeted coupling cavities' center (Fig. 1(b) inset), where a is the photonic crystal lattice constant. Shifting the coupling waveguides further from the CROWL to $6.93 * a$ brings the resonances into sharp contrast and demonstrating the

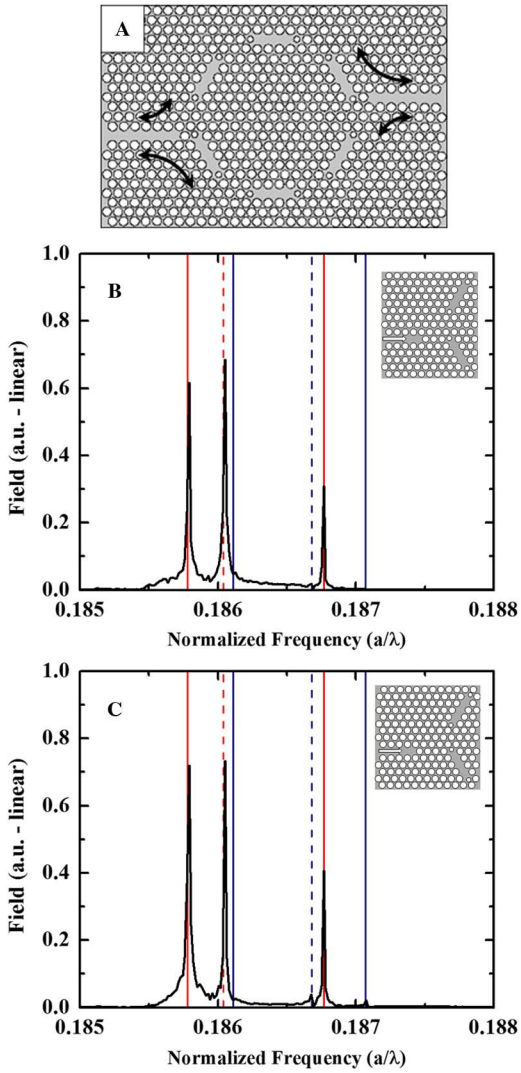

Fig. 9. (color online) Schematic of asymmetric butt-coupling technique for accessing a photonic crystal CROWL (a). FDTD transmission for a waveguide end to cavity center distance of $5.29a$ (b) and $6.24a$ (c).

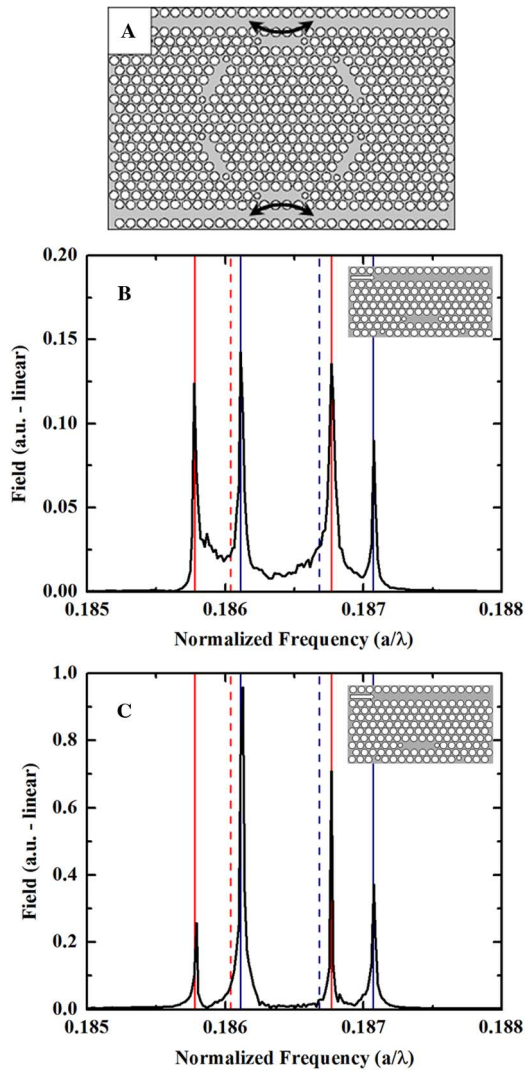

Fig. 10. (color online) Schematic of side-coupling technique for accessing a photonic crystal CROWL (a). FDTD transmission for a waveguide end to cavity center distance of $5.20a$ (b) and $6.06a$ (c).

X-symmetric modes as designated by blue frequency markers in Fig. 8(c).

Exploring physically reasonable alternative geometries in the photonic crystal CROWL backbone, the next waveguide coupling scheme aims to limit coupling to single cavities by shifting the input and output waveguides two crystal rows up or down as illustrated in Fig. 9(a). This coupling method takes the system out of X- or Z-symmetry and so it is referred to as asymmetric butt-coupling. By shifting the input and output waveguides, light will couple more strongly to a single cavity from each waveguide. As predicted by the CMT model, this single-cavity version of butt-coupling yields higher finesse peaks than the symmetric version at the same horizontal spacing. The resolution of these peaks is smaller than that of the FDTD simulation implemented however (15E-6 (a/λ) or 11 GHz at $\lambda = 1.55$ μm) so no quantifiable statement will be made about the specific Q-factors produced at this time. As the waveguides are moved away from the CROWL, the linewidths decrease and transmit the X-antisymmetric modes only (Fig. 9). The reason for X-antisymmetric mode generation is apparent, due to the physical X-asymmetry of the device. It is also worth noting that for waveguide separations smaller than that shown in Fig. 9(b), a resonant structure that transmits all six possible symmetry modes may be achieved.

In order to further limit the waveguide coupling to a single cavity, and to do it in a physically symmetric way, a side coupled scheme was studied. By passing parallel waveguides alongside two opposing cavities as illustrated in Fig. 10(a), guided-mode evanescent coupling is possible. As a note, all spectra shown in his work are normalization to the maximum transmittance of each scheme. Therefore, while it can be said that the device shown in Fig. 10(c) has higher transmittance than that in Fig. 10(b), it is not possible to say how it compares to devices in the other coupling schemes.

Well behaved isolation-like resonances are produced from this scheme, and all have linewidths beneath the FDTD resolution confidence. Side-coupling offers single cavity accessibility which should help to minimize transmitted linewidth, provides simple degree-of-confinement control, and most importantly allows the desired spectral transmission signature. It is therefore

shown to be the most effective method for producing Z-antisymmetric modes and high finesse throughput in this CROWL architecture. Again, for thoroughness, it is noted that for coupling distances smaller than those shown in this work, resonant distortion is observed resulting in an un-desirable resonant structure.

V. Conclusions

Through the study of three different coupling methods for turning a CROWL into a device capable of high Q, multi-peak filtered throughput, the importance of coupling symmetry conditions have become paramount. Using fully numerical techniques, this method of accessing a CROWL quickly brought the work to the practical resolution limit of our FDTD scheme. However, this signifies the potential of coupled-resonator structures, making use of high-Q photonic crystal cavities, for the generation of comb-like, high finesse, passive filtering elements.

Investigation into the modal symmetries that give rise to the resonant groups in CROWLs provides insight that can be used to design these devices with further clarity. The primary barrier to the application of CROW structures to frequency-comb applications remains the uniformity of peak spacing. As the number of coupled-resonators increases, the FSR uniformity for the central resonances increase, and it is expected that engineering the coupling constants will provide for further progress. Future work will be focused on determining the level of resonant control that can be achieved by varying the coupling parameters between neighboring resonators.

References

[1] V. Chaudhery, C. S. Huang, A. Pokhriyal, J. Polans, and B. T. Cunningham, "Spatially selective photonic crystal enhanced fluorescence and application to background reduction for biomolecule detection assays," *Opt. Exp.*, vol. 19, pp. 23327–23340, Nov. 7, 2011.

[2] T. Lei and A. W. Poon, "Modeling of coupled-resonator optical waveguide (CROW) based refractive index sensors using pixelized spatial detection at a single wavelength," *Opt. Exp.*, vol. 19, pp. 22227–22241, Oct. 24, 2011.

[3] S. Yamada, B. S. Song, T. Asano, and S. Noda, "Experimental investigation of thermo-optic effects in SiC and Si photonic crystal nanocavities," *Opt. Lett.*, vol. 36, pp. 3981–3983, Oct. 15, 2011.

[4] C. Sorrentino, J. R. E. Toland, and C. P. Search, "Ultra-sensitive chip scale Sagnac gyroscope based on periodically modulated coupling of a coupled resonator optical waveguide," *Opt. Exp.*, vol. 20, pp. 354–363, Jan. 2, 2012.

[5] B. Ellis, M. A. Mayer, G. Shambat, T. Sarmiento, J. Harris, E. E. Haller, and J. Vuckovic, "Ultralow-threshold electrically pumped quantum-dot photonic-crystal nanocavity laser," *Nature Photon.*, vol. 5, pp. 297–300, May 2011.

[6] Y. Y. Gong, B. Ellis, G. Shambat, T. Sarmiento, J. S. Harris, and J. Vuckovic, "Nanobeam photonic crystal cavity quantum dot laser," *Opt. Exp.*, vol. 18, pp. 8781–8789, Apr. 26, 2010.

[7] S. Matsuo, A. Shinya, T. Kakitsuka, K. Nozaki, T. Segawa, T. Sato, Y. Kawaguchi, and M. Notomi, "High-speed ultracompact buried heterostructure photonic-crystal laser with 13 fJ of energy consumed per bit transmitted," *Nature Photon.*, vol. 4, pp. 648–654, Sep. 2010.

[8] S. Mookherjea, "Semiconductor coupled-resonator optical waveguide laser," *Appl. Phys. Lett.*, vol. 84, pp. 3265–3267, Apr. 26, 2004.

[9] W. H. Zheng, W. J. Zhou, Y. F. Wang, A. J. Liu, W. Chen, H. L. Wang, F. Y. Fu, and A. Y. Qi, "Lateral cavity photonic crystal surface-emitting laser with ultralow threshold," *Opt. Lett.*, vol. 36, pp. 4140–4142, Nov. 1, 2011.

[10] B. Corcoran, M. D. Pelusi, C. Monat, J. T. Li, L. O'Faolain, T. F. Krauss, and B. J. Eggleton, "Ultracompact 160 Gbaud all-optical demultiplexing exploiting slow light in an engineered silicon photonic crystal waveguide," *Opt. Lett.*, vol. 36, pp. 1728–1730, May 1, 2011.

[11] P. J. Delfyett, I. Ozdur, N. Hoghooghi, M. Akbulut, J. Davila-Rodriguez, and S. Bhooplapur, "Advanced Ultrafast Technologies Based on Optical Frequency Combs," *IEEE Sel. Topics Quantum Electron.*, vol. 18, pp. 258–274, Jan–Feb. 2012.

[12] L. Razzari, D. Duchesne, M. Ferrera, R. Morandotti, S. Chu, B. E. Little, and D. J. Moss, "CMOS-compatible integrated optical hyperparametric oscillator," *Nature Photon.*, vol. 4, pp. 41–45, Jan. 10, 2010.

[13] C. Agger, T. S. Skovgard, N. Gregersen, and J. Mork, "Modeling of mode-locked coupled-resonator optical waveguide lasers," *IEEE J. Quantum Electron.*, vol. 46, pp. 1804–1812, Dec. 2010.

[14] T. Baba, "Slow light in photonic crystals," *Nature Photon.*, vol. 2, pp. 465–473, Aug. 2008.

[15] N. Ishikura, T. Baba, E. Kuramochi, and M. Notomi, "Large tunable fractional delay of slow light pulse and its application to fast optical correlator," *Opt. Exp.*, vol. 19, pp. 24102–24108, Nov. 21, 2011.

[16] Y. Liu, Z. Wang, M. H. Han, S. H. Fan, and R. Dutton, "Mode-locking of monolithic laser diodes incorporating coupled-resonator optical waveguides," *Opt. Exp.*, vol. 13, pp. 4539–4553, Jun. 13, 2005.

[17] M. Notomi, E. Kuramochi, and T. Tanabe, "Large-scale arrays of ultrahigh-Q coupled nanocavities," *Nature Photon.*, vol. 2, pp. 741–747, Dec. 2008.

[18] S. A. Schulz, L. O'Faolain, D. M. Beggs, T. P. White, A. Melloni, and T. F. Krauss, "Dispersion engineered slow light in photonic crystals: A comparison," *J. Opt.*, vol. 12, Oct. 2010.

[19] A. Yariv, Y. Xu, R. K. Lee, and A. Scherer, "Coupled-resonator optical waveguide: A proposal and analysis," *Opt. Lett.*, vol. 24, pp. 711–713, Jun. 1, 1999.

[20] M. L. Cooper, G. Gupta, M. A. Schneider, W. M. J. Green, S. Assefa, F. N. Xia, Y. A. Vlasov, and S. Mookherjea, "Statistics of light transport in 235-ring silicon coupled-resonator optical waveguides," *Opt. Exp.*, vol. 18, pp. 26505–26516, Dec. 6, 2010.

[21] T. J. Karle, Y. J. Chai, C. N. Morgan, I. H. White, and T. F. Krauss, "Observation of pulse compression in photonic crystal coupled cavity waveguides," *J. Lightw. Technol.*, vol. 22, pp. 514–519, Feb. 2004.

[22] H. C. Liu and A. Yariv, "Synthesis of high-order bandpass filters based on coupled-resonator optical waveguides (CROWs)," *Opt. Exp.*, vol. 19, pp. 17653–17668, Aug. 29, 2011.

[23] H. C. Liu and A. Yariv, ""Ideal" optical delay lines based on tailored-coupling and reflecting, coupled-resonator optical waveguides," *Opt. Lett.*, vol. 37, pp. 1964–1966, Jun. 1, 2012.

[24] M. D. Weed, C. Williams, P. Delfyett, and W. V. Schoenfeld, "Feedback in coupled-resonance optical waveguides," *Proc. OSA CLEO*, 2012, p. CM3M.4.

[25] J. K. S. Poon, J. Scheuer, and A. Yariv, "Wavelength-selective reflector based on a circular array of coupled microring resonators," *IEEE Photon. Technol. Lett.*, vol. 16, pp. 1331–1333, May 2004.

[26] S. V. Boriskina, "Spectrally engineered photonic molecules as optical sensors with enhanced sensitivity: A proposal and numerical analysis," *J. Opt. Soc. Amer. B Opt. Phys.*, vol. 23, pp. 1565–1573, Aug. 2006.

[27] L. Chremmos and N. Uzunoglu, "Properties of regular polygons of coupled microring resonators," *App. Opt.*, vol. 46, pp. 7730–7738, Nov. 1, 2007.

[28] J. Scheuer and A. Yariv, "Sagnac effect in coupled-resonator slow-light waveguide structures," *Phys. Rev. Lett.*, vol. 96, Feb. 10, 2006.

[29] B. Z. Steinberg, "Rotating photonic crystals: A medium for compact optical gyroscopes," *Phys. Rev. E*, vol. 71, May 2005.

[30] V. Van, "Dual-mode microring reflection filters," *J. Lightw. Technol.*, vol. 25, pp. 3142–3150, Oct. 2007.

[31] M. Sumetsky and B. J. Eggleton, "Modeling and optimization of complex photonic resonant cavity circuits," *Opt. Exp.*, vol. 11, pp. 381–391, Feb. 24, 2003.

[32] A. R. A. Chalcraft, S. Lam, B. D. Jones, D. Szymanski, R. Oulton, A. C. T. Thijssen, M. S. Skolnick, D. M. Whittaker, T. F. Krauss, and A. M. Fox, "Mode structure of coupled L3 photonic crystal cavities," *Opt. Exp.*, vol. 19, pp. 5670–5675, Mar. 14, 2011.

[33] S. Declair, T. Meier, A. Zrenner, and J. Forstner, "Numerical analysis of coupled photonic crystal cavities," *Photon. Nanostruct. Fundam. Appl.*, vol. 9, pp. 345–350, Oct. 2011.

[34] A. Faraon, E. Waks, D. Englund, I. Fushman, and J. Vuckovic, "Efficient photonic crystal cavity-waveguide couplers," *Appl. Phys. Lett.*, vol. 90, Feb. 12, 2007.

[35] M. Qiu, "Effective index method for heterostructure-slab-waveguide-based two-dimensional photonic crystals," *Appl. Phys. Lett.*, vol. 81, pp. 1163–1165, Aug. 12, 2002.

Matthew D. Weed (S'12) received the B.S. degree in physics from Rensselaer Polytechnic Institute, and M.S. degree in Optics from CREOL, the College of Optics and Photonics at University of Central Florida, Orlando, FL, USA, where he is currently pursuing the Ph.D. degree.

General research efforts involve the design and simulation of fabrication-focused photonic structures toward the realization of integrated Quantum Information devices, laser sources, and optical circuitry. Currently, he is focused on the design of Coupled-Resonator Optical Waveguides (CROWs) in Photonic Crystal networks that make use of slow-light phenomena to achieve on-chip mode-locked lasers, optical buffers, and bio-chemical sensors.

Charles G. Williams (S'06) received the B.S. degree in physics from the University of Missouri—Rolla, MO, USA, in 2006 and the M.S. degree in Optics from the University of Central Florida, Orlando, FL, USA, in 2008.

He is currently a Graduate Student with the University of Central Florida in the College of Optics and Photonics, CREOL and FPCE. His research is centered on the creation of low-noise oscillators and optical comb sources for communications, laser ranging, and signal processing-namely through the use of injection locking techniques.

Mr. Williams is a student member of IEEE Photonics Society.

Peter J. Delfyett (S'79–M'94–SM'96–F'02) received the Ph.D. degree in electrical engineering from the City University of New York, NY, USA, in 1988.

He then joined Bell Communication Research as a member of the Technical Staff, where he concentrated his efforts toward generating ultrafast high-power optical pulses from semiconductor diode lasers, for applications in applied photonic networks. He joined the faculty at CREOL—The School of Optics and Photonics of the University of Central Florida, Orlando, FL, USA, in 1993, where he currently holds the positions of University Trustee Chair Professor of optics, electrical and computer engineering, and physics. He has published over 400 articles in refereed journals and conference proceedings and has been awarded 18 U.S. patents.

Dr. Delfyett is a Fellow of the Optical Society of America (OSA) and the IEEE/Lasers and Electro-Optics Society (LEOS), and he is Editor-in-Chief of the IEEE JOURNAL OF SELECTED TOPICS IN QUANTUM ELECTRONICS (JSTQE). He is also the recipient of the National Science Foundation's (NSF's) Presidential Early Career Award for Scientists and Engineers (PECASE) Award and University of Central Florida's Pegasus Professor Award, which is the highest honor awarded by the University.

Winston V. Schoenfeld received the B.S. and M.S. degrees in materials science and engineering from the University of Florida, Orlando, FL, USA, and the Ph.D. degree in materials science from the University of California, Santa Barbara (UCSB), CA, USA, in 2000.

Prior to joining CREOL, he served as Device Manager at Uniroyal Optoelectronics, working in the area of high brightness light emitting diodes (LEDs), and later in 2003 founded Medical Lighting Solutions, Inc., a supplier of specialty LED lighting solutions for the medical and biomedical industries. He has authored/co-authored more than 100 refereed journal publications in the areas of photovoltaics, the epitaxial growth and properties of oxide semiconductors, oxide and nitride-semiconductor light emitting diodes, self-assembled quantum dots, e-beam nano-lithography, quantum information/networks, comprehensive modeling of nanowire devices, and solid-state nuclear material detection.

Dr. Schoenfeld currently serves as Chair of the Florida Chapter of AVS, Principal Editor for the Journal of Materials Research, and Chair of the Micro/Nano-Lithography MOEMS-MEMS conference at SPIE Photonics West.